
Cross section analysis of HQ magnets

Summer Student Internship - Final report

Intern:
Andrea Carbonara

Supervisor:
Eddie Holik

September 25, 2015

Contents

1	Introduction	2
2	Data collection - Single coil	2
2.1	Reference frame identification	2
2.2	Turn location measurement	2
2.3	Numbering scheme and nomenclature for turns and corners	3
2.4	Fitting points to the nominal cross section	3
2.5	Coils analysed	4
3	Turn location analysis	4
3.1	Data processing	4
3.2	Results and plots: cable width	6
3.3	Results and plots: Turn displacement	6
4	Collared data	8
4.1	Current location inside each turn	8
4.2	Field quality results	9
4.3	Cancel first order harmonics	10
4.4	Geometric scaling	10
4.5	Conclusions	10

1 Introduction

The contents of this internship is part of the program of building superconducting magnets for Hi-Lumi LHC upgrade. The main goal of Fermilab Technical Division in this program, as part of LARP association, is to ensure adequate field quality. For this reason a first generation of high-field magnets, called HQ, have been fabricated to test the several aspects of superconducting magnets construction and operation.

For what concerns the internship the goals are two: to collect data about coil cross section in order to quantify turn locations and displacements along the coils and use these data to assess the role of conductor location and displacement on field quality, by comparing actual field measurements with simulation conducted on the basis of collected data about turn locations.

This final report has to be intended as an appendix to the internship final presentation, explaining with more detail the methods used to collect and process data and present and discuss some of the results, for the benefit of the group I worked in. For further clarification and reporting mistakes, please refer to the author at andrea.carbonara@mail.polimi.it

2 Data collection - Single coil

This paragraph wants to describe the steps for measuring turn location for a single coil. The instrument used was an Optical Comparator (Optical Gauging Products), which can measure and store the 2D position of points on a plane with a systematic error less than 0.003mm. The random error, computed as a 1-sigma distance from average from repeated measurements of the same coil cross section, is 0.012mm.

2.1 Reference frame identification

First step after positioning the coil segment on the instrument is to collect data about the outer diameter (from now on, OD) and the keyway sides by an automatic edge detection feature built in the instrument. It collected data on the edges with a spacing of 0.254mm. Points on the OD were used to define the center of the reference frame, by fitting the points to a circle of imposed radius $R = 91.472\text{mm}$. The center of the circle is found by minimising

$$\min_{x_0, y_0} \sum_i (x_i - x_0)^2 + (y_i - y_0)^2 - R^2 \quad (1)$$

being x_0 and y_0 the two variables wrt minimise, representing the circle center, x_i and y_i each collected point on the OD and R the imposed radius of the best fit circle.

The points of the keyway where used to define a 45 deg line in the first quadrant of the reference frame. The line was defined by two points: the center of the reference frame (defined by the OD points) and the center of the keyway, defined as the midpoint between the barycenters of the two sides of the keyway. The barycenter of each side is computed as the average of the coordinates of the point of the side itself.

Once input the center and the location of the point identifying the 45 deg line in the comparator routine, each point collected later on is stored with its position in the new reference frame.

2.2 Turn location measurement

For each turn, the points collected were the four corners. A protractor with perpendicular lines was used to identify the corner in the following way: first, pushing one line to be tangent to the longer edge of the cable and then, keeping that line in that direction, moving the protractor until the second line was tangent to one strand of the shorter edge. In this process, some issues were encountered due to: not perfect alignment of strands,

not perfectly sharp edge of strands, increased cable thickness from the second/third strand due to insulation layer between the strands, strand triplets at some turn edges, with the last or the two last strands being shifted in.

2.3 Numbering scheme and nomenclature for turns and corners

Turns under the 45 deg line are referred to as Non-Transition side turns and turn over the line are to as Transition side turns. Turns are distributed over two layers, the internal being defined as Layer 1 and the external as Layer 2. Turns for NT side are numbered from 1 to 46, starting from L1 turns from midplane to pole, then L2 turns from midplane to pole. Turns for T side are numbered from 47 to 92, starting from L1 turns, from midplane to pole and then L2 turns, from midplane to pole. Each of the four sector is divided in two groups by the wedge. The four corners are ordered as in the picture.

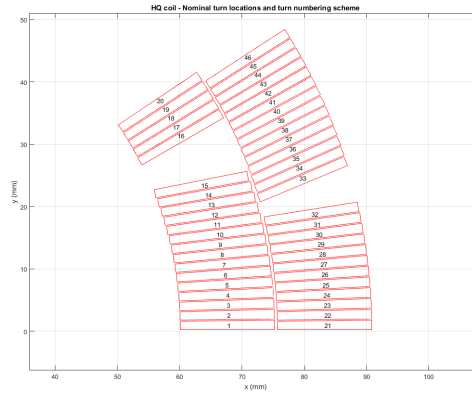


Figure 1: Transition side turns numbering scheme

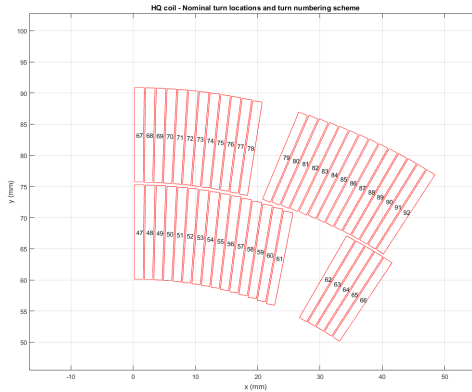


Figure 2: Non-Transition side turns numbering scheme

2.4 Fitting points to the nominal cross section

It started from the evidence that, when comparing the two sides of a single cut, turns didn't overlay but points had a systematic average shift of 0.150mm, suggesting that the process of setting the reference frame according to the OD points was not repeatable for different cross sections. (It turned to be enough repeatable when applied to the same coil, giving the center point with a SD of about 0.010mm).

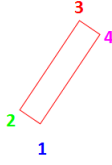


Figure 3: Transition side turns corner order

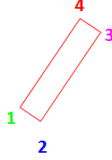


Figure 4: Non-Transition side turns corner order

The process of fitting points to a nominal cross section turned to provide better results when comparing the two sides of a single cut.

In order to modify points to fit the nominal cross section a rigid rototranslation was applied to points and a residual was minimised wrt a rigid translation of (x_0, y_0) and a rotation of θ . The residual minimised is

$$\min_{x_0, y_0, \theta} \sum_i (x_{2,i} - x_{i,nom})^2 + (y_{2,i} - y_{i,nom})^2 \quad (2)$$

$$x_{2,i} = x_{1,i} \cos(\theta) + y_{1,i} \sin(\theta) \quad (3)$$

$$y_{2,i} = -x_{1,i} \sin(\theta) + y_{1,i} \cos(\theta) \quad (4)$$

$$x_{1,i} = x_i + x_0 \quad (5)$$

$$y_{1,i} = y_i + y_0 \quad (6)$$

being x_i, y_i each collected point.

2.5 Coils analysed

Data for single, uncollared coils is available for HQ17 and HQ20 coils @ $z = -5, -105, -205$. Z is the axis of the bore. It origins at the midplane of the magnet and points towards the lead end.

For each coil, data for turn locations and for the datum (OD and keyway sides) is available.

Moreover, for each coils data is available as collected (FirstRefFrame) and after fitting the point to the nominal cross section (FitToNom).

3 Turn location analysis

3.1 Data processing

For each coil cross section, several data has been calculated: cable radial and azimuthal displacement wrt the nominal cross section, cable width and expansion during heat treatment, cable thickness. Each calculation is performed also on the nominal HQ02 cross section, to allow for calculating differences between measured coils and the nominal one.

Minor and major edge midpoint For each turn, the midpoint of the minor edge (the internal one) and the major edge (the external one) was calculated. In the formulas, corners numbers follow the scheme reported above.

$$x_{MinEdge,Mdp} = \frac{x_1 + x_2}{2} \quad (7)$$

$$y_{MinEdge,Mdp} = \frac{y_1 + y_2}{2} \quad (8)$$

$$x_{MajEdge,Mdp} = \frac{x_3 + x_4}{2} \quad (9)$$

$$y_{MajEdge,Mdp} = \frac{y_3 + y_4}{2} \quad (10)$$

$$(11)$$

Midpoint displacements For each midpoint, the displacement wrt the nominal cross section is computed. The displacement is computed in the radial and azimuthal direction, instead of x and y direction. To do that, the position of each midpoint is transformed in polar coordinates according to:

$$R = \sqrt{x^2 + y^2}$$

$$\theta = \text{atan2}(y, x) \quad ^1$$

Then the displacement wrt nominal is calculated between the polar coordinates.

$$\Delta R = R_i - R_{i,nom}$$

$$\Delta \theta = \theta_i - \theta_{i,nom}$$

$$\Delta \theta_{dist} = \Delta \theta R_i$$

Finally, for each midpoint the azimuthal displacement is multiplied by the radial position of the corresponding midpoint in the nominal cross section, in order to have a distance unit for the displacement. So the final azimuthal displacement IS NOT a difference of angular position of the two points but IT IS an actual displacement in the normal direction. Note that the displacement is positive from midplane to pole, so its positive direction is different according to the turn being in the T or NT side.

Cable width and expansion Cable width is computed as the distance between the two midpoints. Cable expansion is computed as follows. The reference width is referred to a condition pre-heat treatment: $w_{ref} = 14.78mm$ for each turn and coil.

$$\%exp = \frac{w - w_{ref}}{w_{ref}} 100$$

Cable thickness Cable thickness is computed for both minor edge and major edge, as follows:

- Take the line perpendicular to that one passing through the two midpoints
- Take the line connecting corner 1 to 4 and 2 to 3 of the turn (the two longer edges of a turn)
- Intersect the line at first point with the two at second point
- Compute the distance between the two intersection points

This way is independent of any kind of deformation of the turn.

3.2 Results and plots: cable width

In the following plots the turn number is shown on ascissa, according to the numbering scheme reported above. Black dotted lines represent the wedges and the position of the midplanes and the pole is reported. The turn is divided in four blocks being Transition/Non-Transition side Layer 1/Layer 2. The different colors represent a different coil cross section, according to the legend.

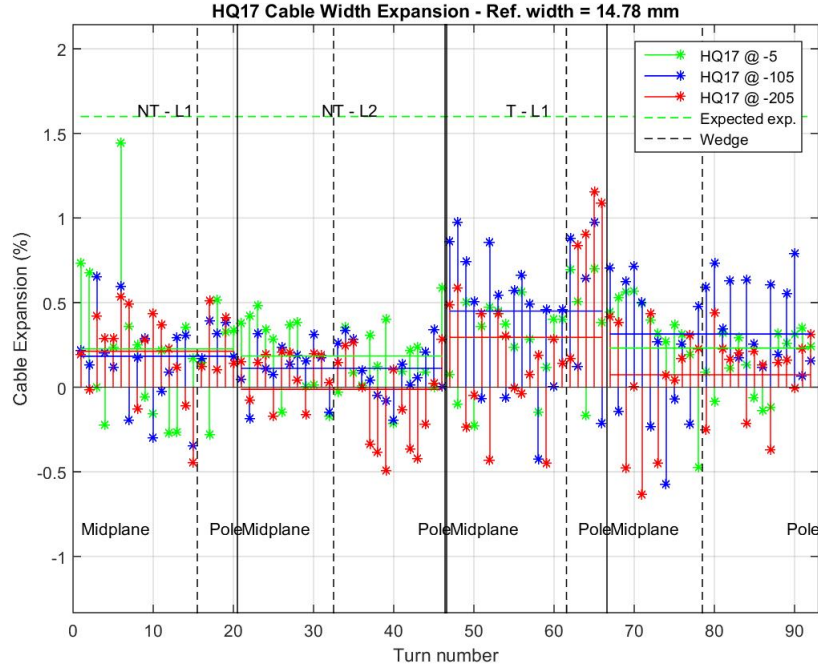


Figure 5: HQ17 Cable relative expansion during heat treatment - Braided on insulation

The plots clearly show the different level of expansion between HQ17 and HQ20, the first using a cable with braided on insulation, the second using a cable with a sock insulation. The braided on insulation constricts more the cable and allows for minor expansion during heat treatment. Moreover, variance of expansion between each turn is much less for HQ17.

Statistical significance of the difference between the two coils is evaluated. The average expansion and the standard deviation is computed for each of the two coil. The averages difference turns to be more than twice the difference standard deviation (computed with the RSS rule), signal of statistical evidence of the difference being different from zero.

As a secondary effect, the difference between expansion in layer 1 and in layer 2 has been investigated for the two coils, but there was no statistical evidence for that.

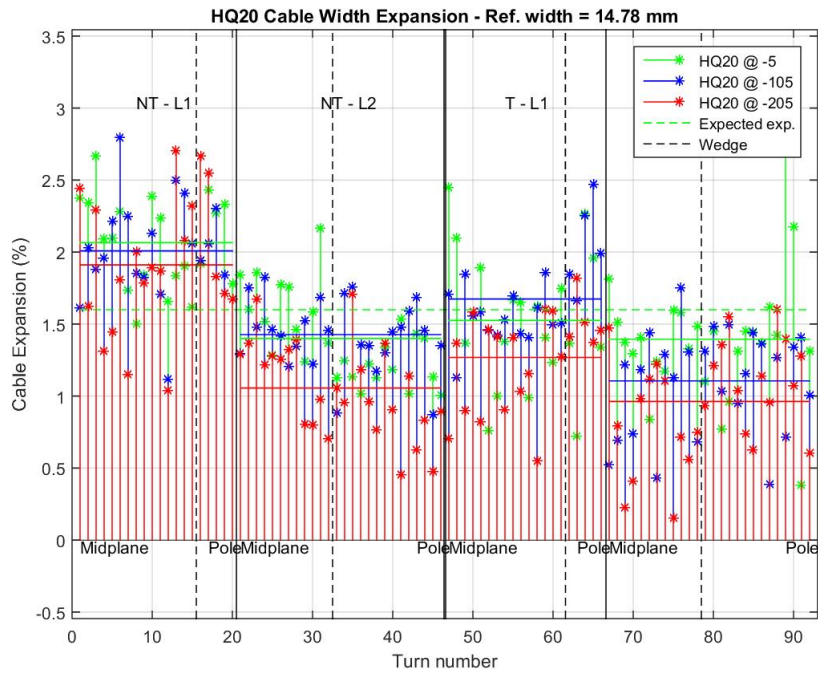


Figure 6: HQ20 Cable relative expansion during heat treatment - Sock insulation

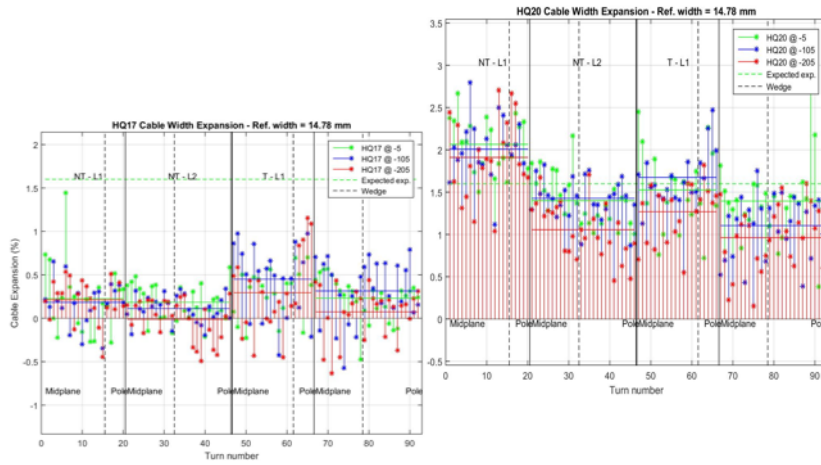


Figure 7: HQ17-20 Cable relative expansion comparison

	HQ17		HQ20		Difference	
	Avg	Sd	Avg	Sd	Diff.	Sd
Expansion (%)	0.37	0.32	1.64	0.50	1.27	0.60

Figure 8: HQ17-20 Average cable expansion difference - Statistical evidence

	NT - L1		NT - L2		Difference		T - L1		T - L2		Difference	
	Avg	Sd	Avg	Sd	Diff.	Sd	Avg	Sd	Avg	Sd	Diff.	Sd
HQ17	0.21	0.31	0.10	0.22	0.11	0.38	0.35	0.39	0.21	0.32	0.14	0.50
HQ20	1.20	0.39	1.29	0.34	0.70	0.52	1.49	0.41	1.16	0.44	1.34	0.60

Figure 9: L1/L2 Cable expansion difference - No Statistical evidence

3.3 Results and plots: Turn displacement

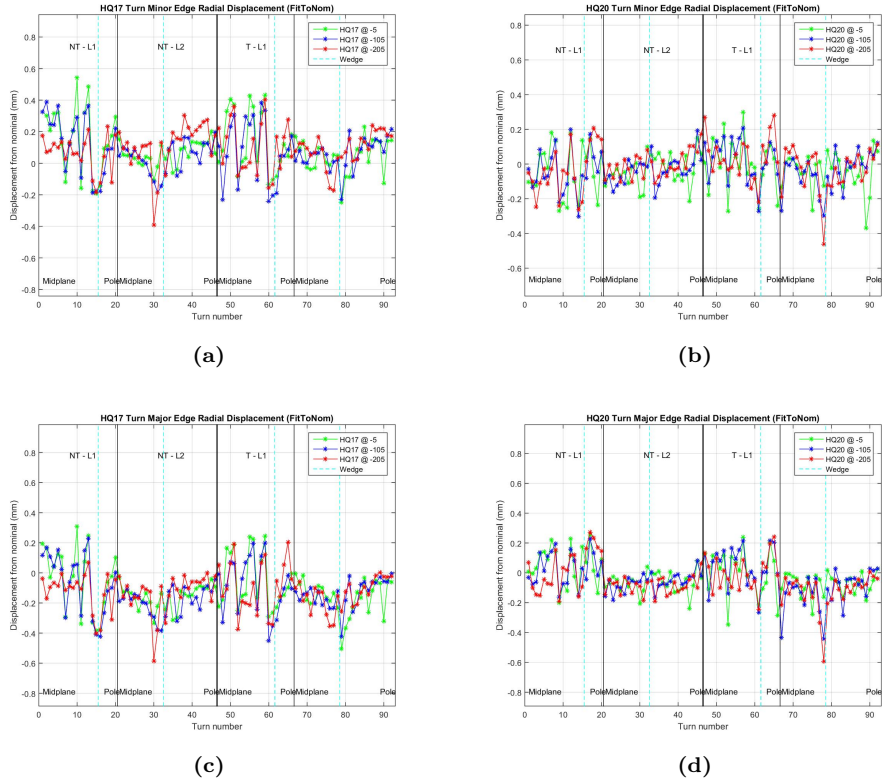


Figure 10: HQ17 and HQ20 Radial displacement

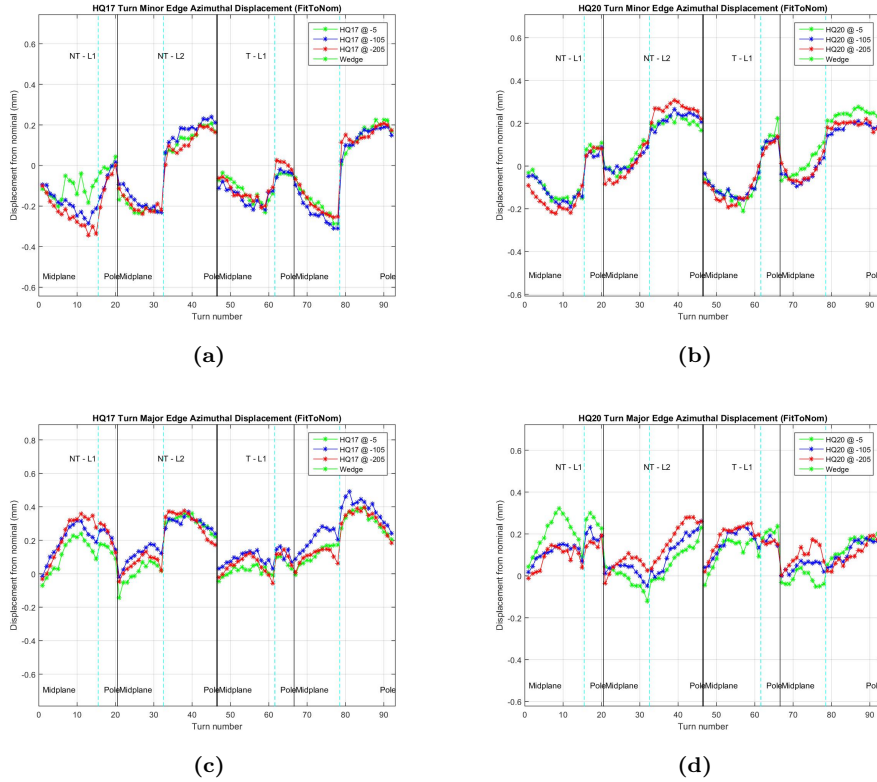


Figure 11: HQ17 and HQ20 Azimuthal displacement

Plots show radial and azimuthal displacement for minor and major edge midpoint for coils HQ17 and HQ20 at the three different cross sections. Radial displacement is quite a noisy signal because also adjacent turns are radially shifted because of the winding process. Azimuthal displacement is continuous, jumps being at wedges, which azimuthally push turns.

Azimuthal displacement at the midplane turns show how coils are shifted outward when they are not constrained by the collars. Turn variance over the span of 20cm is up to 0.200mm for azimuthal displacement and up to 0.300mm for radial displacement.

Many points look as outliers, but actually they aren't because they have been further investigated with the comparator and because some points with exceptional displacement show the same behaviour for both minor edge and major edge (which are measured independently).

4 Collared data

Three full cross section have been assembled using coils HQ17, HQ16, HQ15, HQ20 from the first quadrant counterclockwise. The four coils have been assembled with four collars, meeting the requirement of 100 in-lb torque for bolts. The cross section analyzed were at $z = -5, -79, -105$. $z = -79$ cross section is seen from trailing end of the magnet, so points have been flipped around the 45 deg line to be comparable with other cross sections.

All previous consideration apply to the process of collecting data points, except for the reference frame setting: the keyway sides of the four coils were used. For each keyway the center was computed as mentioned before and the center of the reference frame was set at the intersection of the line passing through opposite keyway centers.

The computations about cable width, expansion, displacements and thickness was made also for collared coils HQ17 and HQ15 (first and third quadrant, so the coils with nominally the best alignment of the pole with the chosen reference frame).

4.1 Current location inside each turn

In order to use the measured turn locations to compute magnetic field, the position of the currents has been computed. The cable is supposed to have 36 strands, divided in two rows with 18 strand each, equally distant each other and from the turn corners. The actual process of finding the current locations is the following:

$$\mathbf{P}_{1j} = \frac{1}{4}(2j-1)\mathbf{x}_1 + (1 - \frac{1}{4}(2j-1))\mathbf{x}_2 \quad j = 1, 2$$

$$\mathbf{P}_{2j} = \frac{1}{4}(2j-1)\mathbf{x}_3 + (1 - \frac{1}{4}(2j-1))\mathbf{x}_4$$

$$\mathbf{x}_{ij} = \mathbf{P}_{1j} + \frac{(\mathbf{P}_{2j} - \mathbf{P}_{1j})}{36}(2i-1) \quad i = 1, \dots, 18$$

4.2 Field quality results

The following are results for multipoles measured at $z = -5$ and -105 and computed at $z = -5, -79, -105$.

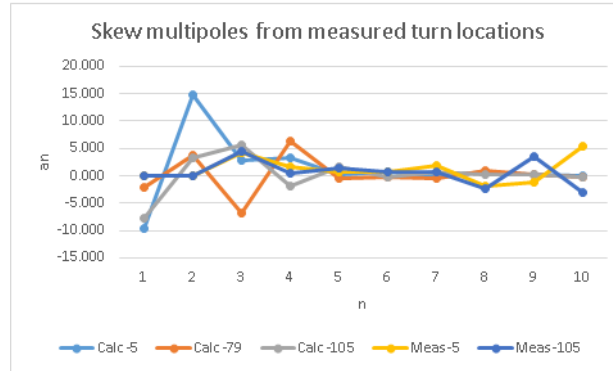


Figure 12: Field quality results - skew multipoles

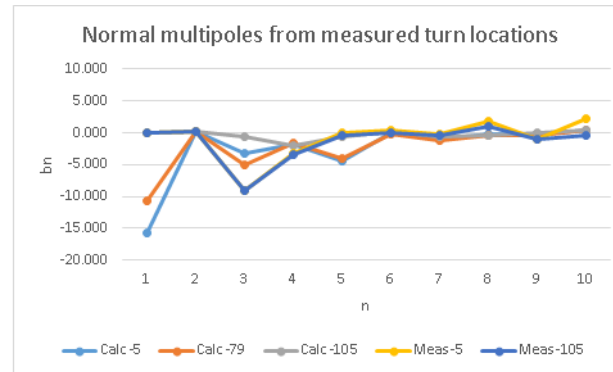


Figure 13: Field quality results - normal multipoles

4.3 Cancel first order harmonics

4.4 Geometric scaling

To compensate the fact that assembled collars is not perfectly square as it should be, points have been scaled as follows. The top-bottom and left-right d_1 and d_2 sides of the fully assembled cross section have been measured. The assembly turned to be larger than

how much tall it was, so points have been scaled down in the x direction and scaled up in the y direction in order for both sides to meet the average of the measured distances.

Scaling factor k is calculated wrt the nominal OD of the coil (considering rigid the collar), as

$$k = \frac{OD + \frac{d_2 - d_1}{2}}{OD}$$

4.5 Conclusions

Numerical results for field quality actually don't match experimental measurements. Possibly the reason is the turn location variance along the coils is too large to compare a single cross section with measurements taken averaging results over a 10cm span.

The application of correction about first order harmonics and geometric scaling affected multipoles less than 1/1000.